Fracture Mechanics of Concrete and Concrete Structures -
Assessment, Durability, Monitoring and Retrofitting of Concrete Structures- B. H. Oh, et al. (eds)
 ISBN 978-89-5708-181-5

Rebar bond slip in diagonal tension failure of reinforced concrete beams

T. Hasegawa
Institute of Technology, Shimizu Corporation, Tokyo, Japan

ABSTRACT: The influence of modeling of rebar bond slip on diagonal tension failure of reinforced concrete beams in finite element analysis is examined through calculations with several modeling strategies for bond slip and bond splitting fracture. The elasto-plastic constitutive model with dilatancy in bond interface elements results in extensive bond splitting cracking and further propagation of the diagonal cracks connected to the bond splitting cracks. The partial debonding model between concrete and rebar beam elements can simulate the diagonal tension failure mode depending on the configuration of debonding nodes.

1 INTRODUCTION

Diagonal tension failure of reinforced concrete structures is influenced by many factors such as mixed mode fracture of concrete, localization and propagation of diagonal cracks, longitudinal splitting cracks along tension rebars, fracture bifurcation, constitutive relations of concrete, rebar bond slip, and dowel action of rebar. Those factors have to be taken into account to simulate the failure mechanism of the structures for rational shear design of reinforced concrete structures. In previous studies (Hasegawa 2004 and Hasegawa 2007a) finite element analysis of diagonal tension failure in a reinforced concrete beam was performed using the Multi Equivalent Series Phase Model (MESP Model; Hasegawa 1998), and the failure mechanisms were discussed by analyzing the numerical results. In the analysis, branch-switching for fracture bifurcation, influence of concrete crack models, mixed mode fracture, and mesh dependency were focused on and examined. Among the other influencing factors not examined in the previous studies, in particular rebar bond slip and longitudinal splitting fracture are considered to be quite important and difficult to examine in both experimental and numerical investigations. The bond slip of reinforcing bars is considered to influence the failure through the mechanism that the bond slip increases the width of diagonal cracks and changes the propagation of the cracks to unstable propagation. The bond slip also causes splitting cracks of concrete cover along the reinforcing bar, that connect with diagonal cracks, and it results in a trigger of diagonal tension collapse of the beam in an unstable manner. In this study (Hasegawa 2007b, 2008, and 2009) the influence of modeling of rebar bond slip on diagonal tension failure of reinforced concrete beams in finite element analysis is examined through calculations with several modeling strategies for bond slip and bond splitting fracture.

2 BOND STRESS-SLIP MODELS

Rebar bond slip is usually simulated by using interface elements with a bond stress τ - slip S relationship such as Eq. 1 (Witte & Kikstra 2007) in finite element analysis of reinforced concrete structures. However, the bond stress-slip relationships obtained from pullout test experiments of reinforced concrete are known to be not unique but strongly depend on the boundary conditions in the experiments, such as embedded length of the rebar, distance of the measurement position

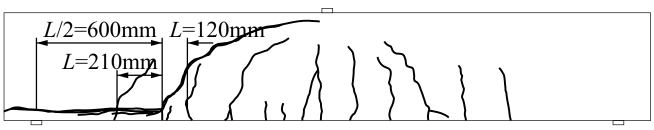

Figure 1. Experimental cracking pattern of BN50 after failure.

Table 1. Models for bond stress-slip relationship.

Model	Length L of pullout specimen (mm)	Location $2x/L$	τ - S or □| S| ε_s equation	Bond strength (N/mm^2)
b-1	Non	Non	Eq. 1	3.80
b-2	120	0.50	Eq. 2	2.90
b-3	210	0.50	Eq. 2	4.81
b-4	210	0.50	quarter stiffness of model b-3	4.81
b-5	120	0.75	Eq. 2	1.47

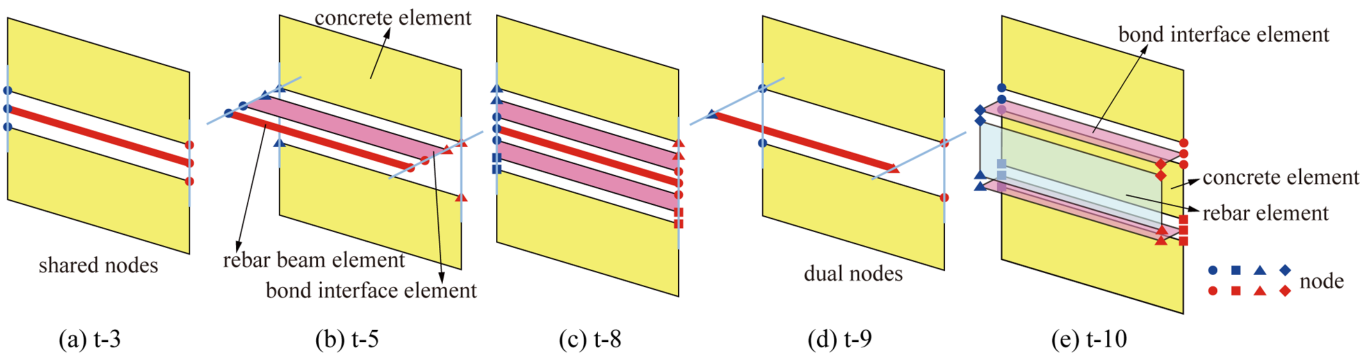

Figure 3. Tension models in RC beams.

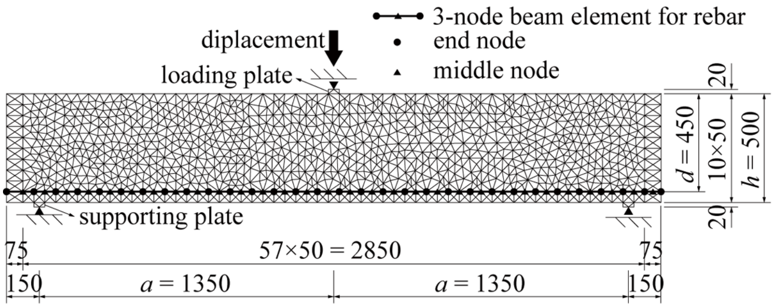

Figure 4. Finite element mesh for concrete and rebar.

from the pullout end, and so on. To circumvent this problem the bond stress τ - slip S - rebar strain ε_s relationship of Shima (Shima, Chou & Okamura 1987), Eq. 2 is utilized, which does not depend on the boundary conditions in pullout test of rebar. However, it is difficult to take the rebar strain into account in ordinary interface finite elements. To simulate diagonal tension failure of a reinforced concrete slender beam, experimental specimen BN50 tested at the University of Toronto (Podgorniak-Stanik 1998), the flexural tension part of the beam was considered to be capable of being modeled into pullout specimens of the lengths L = 1200, 210, 120 mm, see Figure 1. The integral equation for slip, Eq. 3, and the differential equation for bond stress, Eq. 4, are numerically solved for the assumed pullout specimens having their lengths L of 1200, 210, and 120 mm, together with the bond stress-slip-rebar strain relationship, Eq. 2. From the numerical analysis, bond stress $\tau(x)$-slip $S(x)$ relationships at any location x are obtained, which take into account the lengths of the pullout specimens, i.e., crack spacings of the reinforced concrete beam.

$0 \le S < S^0$:

$$\tau = f_t\left[5\left(S/S^0\right) - 4.5\left(S/S^0\right)^2 + 1.4\left(S/S^0\right)^3\right] \quad (1a)$$

$S \ge S^0$:

$$\tau = 1.9 f_t \quad (1b)$$

$$\frac{\tau}{f_c'} = \frac{0.73\left[\ln\left(1 + 5000 S/D\right)\right]^3}{1 + \varepsilon_s \times 10^5} \quad (2)$$

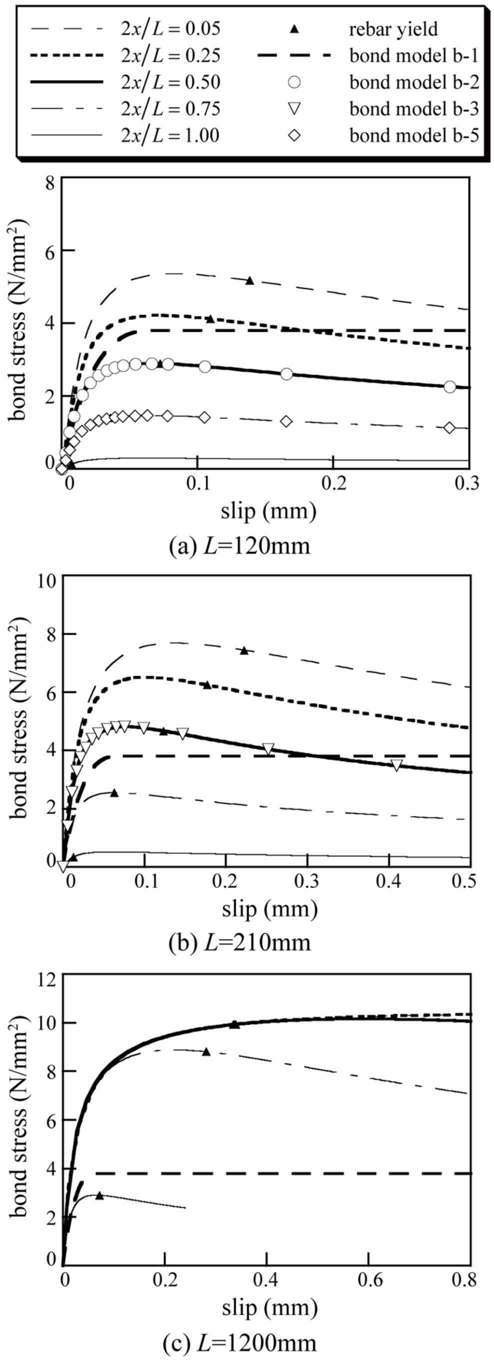

Figure 2. Bond stress-slip relationship.

$$S(x) = \int_{x_0}^{x} \varepsilon_s(x)\,dx + S(x_0) \quad (3)$$

Table 2. Analysis cases.

Analysis case	Tension model	Bond interface element	Number of disconnected nodes for rebar	Bond slip constitutive model	$\tau - S$ relationship	$\tan\phi = \tan\psi$
A05	t-3	Not used	Non	Non	Non	Non
A06	t-5	Used	Non	$\tau - S$ relationship only	b-1	Non
G01	t-5	Used	Non	$\tau - S$ relationship only	b-2	Non
G02	t-5	Used	Non	$\tau - S$ relationship only	b-3	Non
G03	t-5	Used	Non	$\tau - S$ relationship only	b-4	Non
G04	t-8	Used	Non	$\tau - S$ relationship only	b-2	Non
G05	t-5	Used	Non	$\tau - S$ relationship only	b-5	Non
H01	t-3 and t-9	Not used	3	Non	Non	Non
H02	t-3 and t-9	Not used	41	Non	Non	Non
H03	t-3 and t-9	Not used	30	Non	Non	Non
H04	t-3 and t-9	Not used	13	Non	Non	Non
H05	t-3 and t-9	Not used	10	Non	Non	Non
I01	t-10	Used	Non	$\tau - S$ relationship only	b-3	Non
I02	t-10	Used	Non	Coulomb friction model	b-3	0.5
I03	t-10	Used	Non	Coulomb friction model	b-3	1.0
I04	t-10	Used	Non	Coulomb friction model	b-3	1.5
I05	t-10	Used	Non	Coulomb friction model	b-3	2.0

$$\tau(x) = \frac{D}{4}\frac{d\sigma_s\left(\varepsilon_s(x)\right)}{dx} \tag{4}$$

where $\tau(x)$ = bond stress at x; $S(x)$ = slip at x; $\varepsilon_s(x)$ = rebar strain at x; f_t = tensile strength of concrete; f_c' = compressive strength of concrete; D = diameter of rebar; x = location coordinate of pullout specimen with its origin x_0 at the center of the specimen.

Figure 2 shows the calculated bond stress $\tau(x)$ - slip $S(x)$ relationships at location x for each L. As indicated in the calculation results, bond stress-slip relationships for reinforced concrete beams are not unique but depend on the location and dramatically alter as a result of the change of the boundary condition (crack spacing) with cracking. It is not reasonable to define a unique τ-S relationship, however, more appropriate τ-S-ε_s relationships are difficult to implement in the ordinary finite element method without nonlocal formulation. Therefore, in the first series A and G of analysis cases, bond models b-1, b-2, b-3, b-4, and b-5 as average bond stress-slip relationships are assumed as shown in Table 1 and Figure 2. Analysis cases A06, G01, G02, G03, G04, and G05 are calculated as explained in Table 2. Paying attention to the connection of concrete elements, bond interface elements, and rebar beam elements, tension models t-5 and t-8 as shown in Figure 3 are considered in the analysis. Figure 4 shows the random Delaunay triangulation mesh for concrete elements and 3-node beam elements for rebar in analysis case G. The Multi Equivalent Series Phase Model is assumed in all the analysis cases as the concrete constitutive model.

Figure 5 compares the calculated shear response in analysis cases A05, A06, G02, and G03 with the experiment. In Figure 6 the calculated shear response in analysis cases A05, G01, and G05 are shown. While in analysis case A05 the calculation is done for perfect bonding between concrete and rebar, analysis case G01 assumes the bond model b-2 that is obtained for $2x/L = 0.50$ and has a higher bond strength (2.90 $\mathrm{N/mm^2}$). On the other hand, in analysis case G05 the bond model b-5 is assumed, that is calculated for $2x/L = 0.75$ and has a lower bond strength (1.47 $\mathrm{N/mm^2}$). In all those analysis cases we can not obtain the expected unstable and brittle diagonal tension failure mode due to widening of diagonal crack widths resulted from rebar bond slip, but flexural failure mode. Figures 7, 8 and 9 plot the lines of maximum principal strain $\varepsilon_1 \geq 5\varepsilon_{t0}$ with the thickness proportional to its value in analysis cases A05, G02, and G05. This represents the crack strain and crack direction at maximum shear load V_u, and is a good measure of crack width (ε_{t0} = the tensile strain corresponding to tensile strength). Comparing cracking patterns of analysis cases A05 with perfect bond and G05 with the weak bond model obtained for the position near the pullout end, longitudinal cracks do not occur in the latter case since the force transfer from rebar to concrete is not enough because of weak bond strength. In analysis case G05 diagonal cracking does not develop so much, and cracks concentrate in the middle part of the specimen span, which resembles the tied arch load-carrying mechanism observed in reinforced concrete beams without bond between the rebar and concrete. Compressive failure of arch crown concrete is confirmed at the maximum shear load in analysis

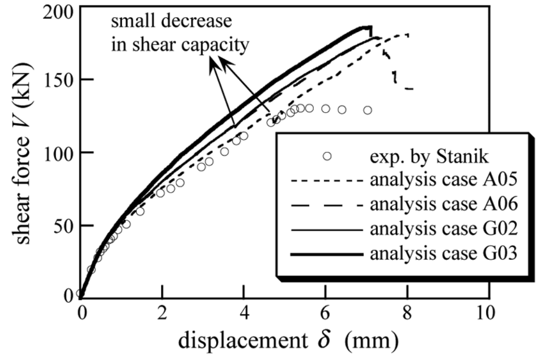

Figure 5. Shear response in analysis case G.

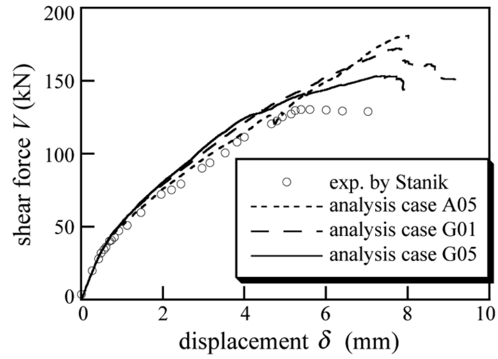

Figure 6. Shear response in analysis cases G01 and G05.

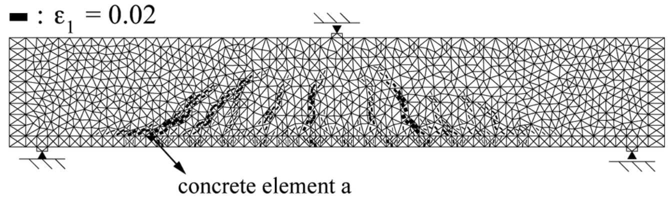

Figure 7. Cracking pattern in analysis case A05.

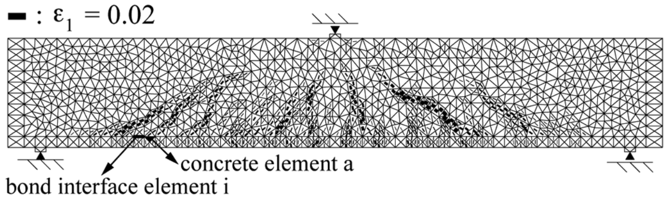

Figure 8. Cracking pattern in analysis case G02.

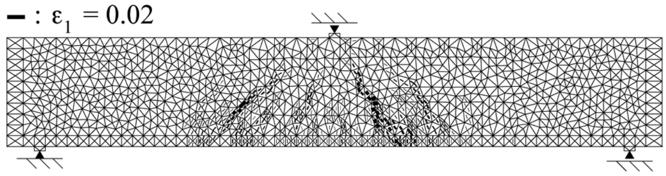

Figure 9. Cracking pattern in analysis case G05.

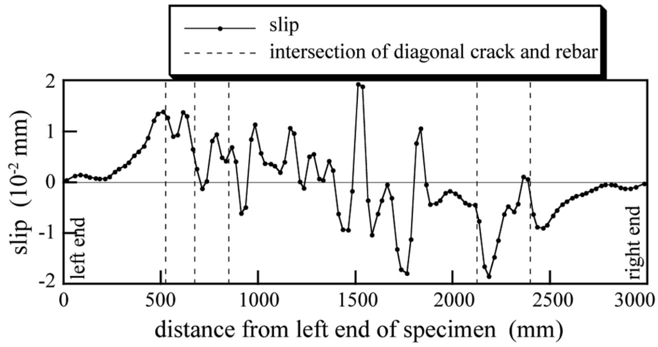

Figure 10. Bond slip distribution in analysis case G02.

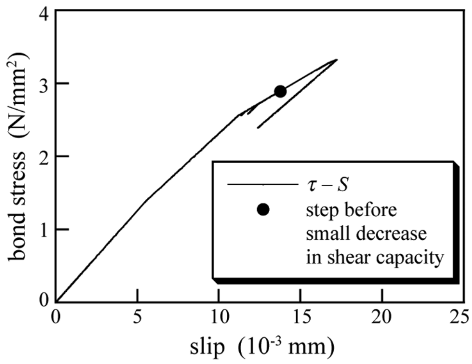

Figure 11. Bond stress-slip response in analysis case G02.

case G05. On the other hand, in analysis case G02, the bond model b-3 with higher bond strength (4.81 $\mathrm{N/mm^2}$) produces a good prediction of the experimental cracking pattern with longitudinal and diagonal cracks.

Figure 10 is the slip distribution in bond interface elements at the step before small decrease in shear capacity (Fig. 5), along with indications of the intersection of diagonal cracks and rebar in analysis case G02. Figures 11 and 12(a) show the bond stress-slip response of interface element i (Fig. 8) and the stress-strain response of concrete element a (Fig. 8), which are located at the intersection of the main diagonal crack and the rebar in analysis case G02. On the other hand Figure 12(b) shows the stress-strain response of concrete element a (Fig. 7) in analysis case A05 without bond slip. The element a is located at a similar point to that in analysis case G02. These results suggest that the rebar bond slip does not increase the width of a certain dominant diagonal crack resulting in localized diagonal tension failure with instability, but tends to homogenize the strain of all cracks along the rebar, which causes stable flexural failure. Use of bond interface elements decreases the force transfer from the rebar to concrete elements, and therefore, suppresses the growth of longitudinal splitting cracks. This results in failure to simulate the complete diagonal tension collapse mechanism.

3 PARTIAL DEBONDING MODEL

In analysis case H some parts of rebar beam elements are arranged to be not connected to concrete elements, simulating partial debonding between concrete and rebar. To trigger an unstable propagation of a dominant diagonal crack, concrete elements in the vicinity of rebar beam elements need to increase their crack strain by being disconnected from the rebar beam elements. For that purpose some parts of concrete elements are arranged not to have

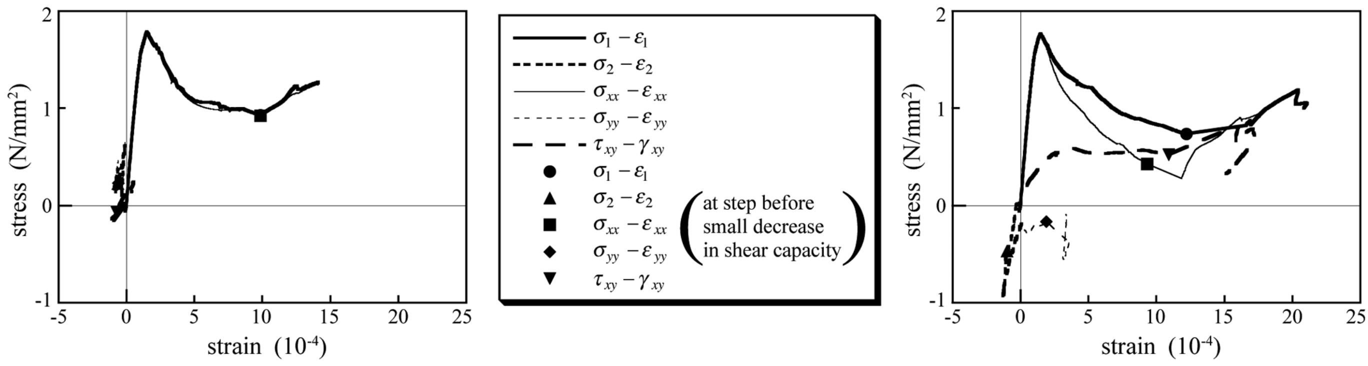

(a) element a in analysis case G02

(b) element a in analysis case A05

Figure 12. Stress-strain responses.

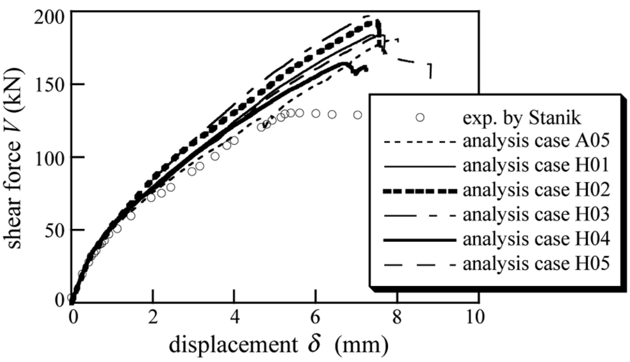

Figure 13. Shear response in analysis case H.

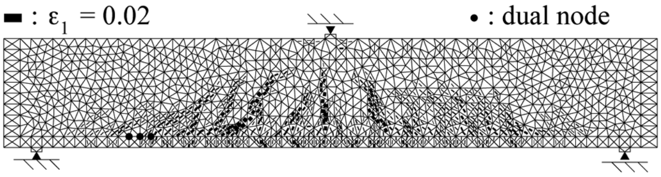

Figure 14. Cracking pattern in analysis case H01.

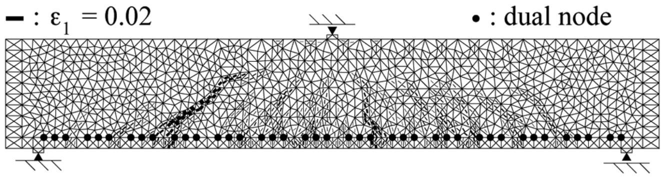

Figure 15. Cracking pattern in analysis case H02.

nodal constraint from the neighboring rebar beam elements by using dual nodes for both elements. Perfect bonding between concrete and rebar beam elements is modeled by using shared nodes for both elements as shown in tension model t-3 (Fig. 3(a)). On the other hand perfect debonding between concrete and rebar beam elements is modeled by using dual nodes for both elements as shown in tension model t-9 (Fig. 3(d)). Finite element models of analysis case H have nodal connectivity according to both the tension models t-3 and t-9 although the meshes for concrete and rebar beam elements are apparently not different from those for analysis case A05 (Fig. 4). The number of dual nodes for concrete and rebar beam elements, i.e., the number of disconnected nodes for rebar beam elements is shown in Table 2 for each analysis case.

Figure 13 shows the calculated shear response in analysis case H for the partial debonding model, compared with the experiment and analysis case A05 for perfect bond. In Figures 14, 15, 16, 17, and 18, cracking patterns at maximum shear load are shown for analysis cases H01, H02, H03, H04, and H05. In these figures the dual nodes for both concrete and rebar beam elements are indicated by solid circles. As explained before, rebar beam elements are disconnected from concrete elements at the dual nodes. The appearances of diagonal, flexural, and longitudinal cracks strongly depend on the positions and numbers of dual nodes. A close examination of cracks in concrete elements around dual nodes and shared nodes reveals that cracks do not necessarily occur at the concrete elements in the vicinity of dual nodes that do not have constraint from the neighboring rebar beam elements. However, lots of cracks occur at the concrete elements having shared nodes with rebar beam elements.

By examining the diagonal crack, cracking pattern, incremental displacement, and yielding of rebar at maximum shear load, diagonal tension failure is clearly confirmed only in analysis case H04, but flexural tension failure mode is observed in analysis cases H01, H02, and H05. In analysis case H03 shear compression or flexural compression failure mode is more dominant rather than diagonal tension or flexural tension failure mode. The incremental displacement at the maximum shear load in analysis case H04 is shown in Figure 19. It is obvious that one dominant diagonal crack propagates towards the lower right side of the loading plate on the upper compressive surface of the reinforced concrete beam, and a diagonal tension collapse mechanism is simulated very reasonably and accurately, as shown also in the cracking pattern of Figure 17. However, it has to be mentioned that important discrepancies are confirmed between the analysis and the experiment, that is, the dominant diagonal crack is not curved but almost straight, and the intersection of the dominant diagonal crack and rebar is closer to the center of reinforced concrete beam, compared with the experiment. Furthermore, longitudinal cracks along the rebar, which are one of

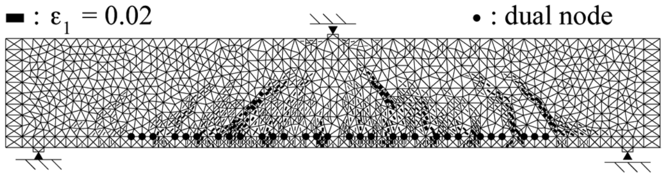

Figure 16. Cracking pattern in analysis case H03.

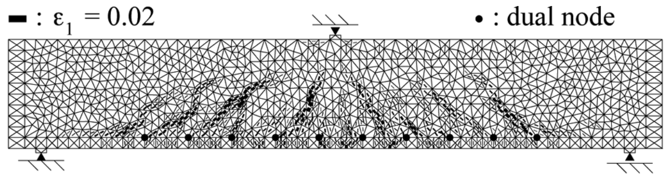

Figure 18. Cracking pattern in analysis case H05.

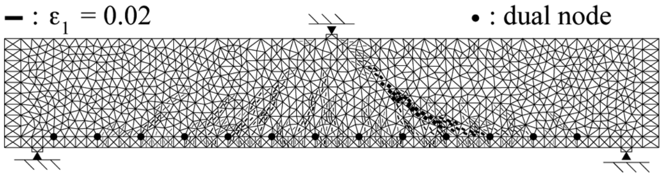

Figure 17. Cracking pattern in analysis case H04.

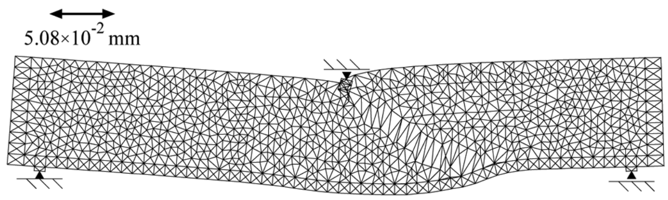

Figure 19. Incremental displacement in analysis case H04.

the primary causes of diagonal tension failure, do not develop much in analysis case H04 due to the weak bond between concrete and rebar beam elements. These discrepancies result in the overestimation of maximum shear load in analysis case H04.

4 BOND SPLITTING FRACTURE MODELING

Since bond splitting cracks or longitudinal splitting cracks, which occur at the level of the tension rebar, usually connect with the dominant diagonal crack and accelerate its propagation, the bond splitting cracks or longitudinal splitting cracks are considered an important trigger of diagonal tension collapse. The bond splitting cracks occur in the concrete cover due to the tensile hoop stress around rebar, which is caused by the radial force from the rib of rebar when the rebar is pulled out from concrete and slips. The rational simulation of the mechanism for bond splitting cracking needs truly three-dimensional meso-level mechanics or micromechanics analysis in which detailed geometrical modeling of the ribs of rebar and surrounding concrete has to be done together with identification of meso-level mechanics properties or micromechanical properties of the materials. The three-dimensional analysis is not that easy since experimental information is lacking. In this study we pursue an expedient method to simulate the mechanism of bond splitting cracking in conjunction with diagonal tension failure under two-dimensional plane stress conditions for simplification. In tension model t-10, concrete elements, rebar plane elements, and bond interface elements are arranged to be connected as shown in Figure 3(e) so that the bond slip in interface elements causes dilatancy in the normal direction of rebar, which induces tensile stress and cracking in the longitudinal direction of concrete elements. For this phenomenological modeling of bond splitting crack, a Coulomb friction elasto-plasticity constitutive model is utilized in the bond interface elements, which is described as in Eqs. 5, 6, and 7.

$$d\mathbf{t} = \begin{bmatrix} D_{nn} & D_{nt} \\ D_{tn} & D_{tt} \end{bmatrix} d\mathbf{u} = \left[\mathbf{D}^e - \frac{\mathbf{D}^e \dfrac{\partial g}{\partial \mathbf{t}} \dfrac{\partial f}{\partial \mathbf{t}}^T \mathbf{D}^e}{h + \dfrac{\partial f}{\partial \mathbf{t}}^T \mathbf{D}^e \dfrac{\partial g}{\partial \mathbf{t}}} \right] d\mathbf{u} \tag{5}$$

$$f = \sqrt{t_t^2} + t_n \tan\phi - c(\kappa) = 0 \tag{6}$$

$$g = \sqrt{t_t^2} + t_n \tan\psi \tag{7}$$

where $\mathbf{t}$ = normal traction t_n and bond traction t_t; $\mathbf{u}$ = normal relative displacement u_n and slip displacement u_t or S; $\mathbf{D}^e$ = elastic stiffness matrix; f = yield function; g = plastic potential function; ϕ = friction angle; ψ = dilatancy angle; $c(\kappa)$ = cohesion; κ = internal parameter or effective plastic strain; h = plastic hardening modulus.

In the case of the bond stress τ - slip S relationship utilized for bond interface elements in most finite element analysis of reinforced concrete, the off-diagonal terms of Eq. 5 are all zero, which means that neither dilatancy nor cross effect is taken into account. The associated flow rule ($f = g$) is assumed for stable calculation. The plastic hardening or effective plastic stress-strain relationship is identified by using the bond model b-3.

In analysis case I the tension model t-10 is used together with the Coulomb friction elasto-plasticity constitutive model in bond interface elements. Figure 20 shows the finite element mesh in analysis case I. Since the dilatancy of the Coulomb friction elasto-plasticity constitutive model influences bond splitting cracking, the analysis is done by assuming various dilatancy angles ψ for each analysis case as shown in Table 2. Figure 21 shows the slip and normal relative displacements obtained in shear test simulation using the Coulomb friction elasto-plasticity constitutive model with various dilatancy angles. It is obvious that normal relative displacement or the dilatancy can be adjusted by the dilatancy angle.

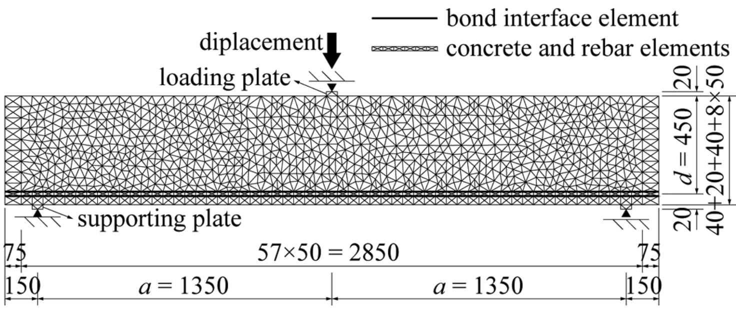

Figure 20. Finite element mesh in analysis case I.

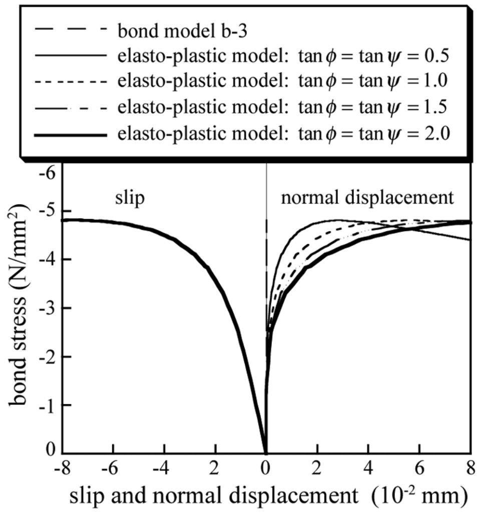

Figure 21. Bond slip constitutive relation.

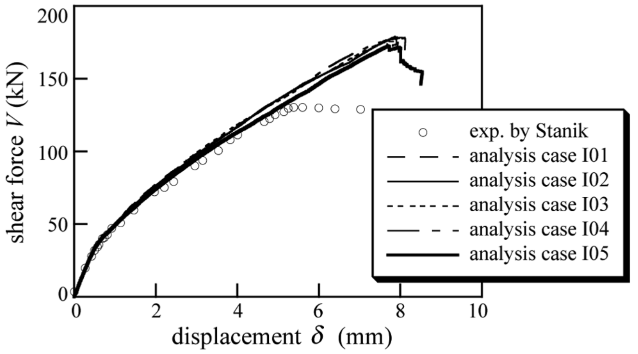

Figure 22. Shear response in analysis case I.

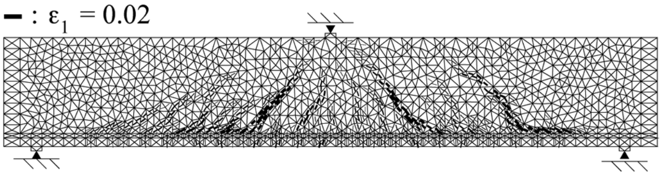

Figure 23. Cracking pattern in analysis case I01.

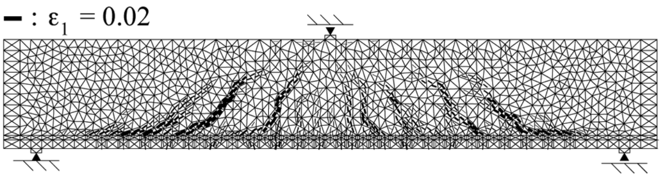

Figure 24. Cracking pattern in analysis case I02.

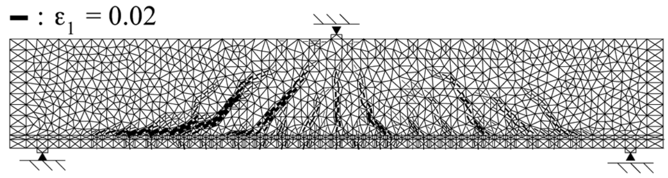

Figure 25. Cracking pattern in analysis case I03.

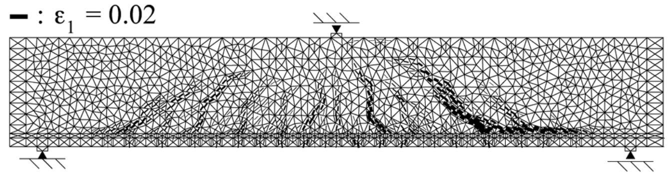

Figure 26. Cracking pattern in analysis case I04.

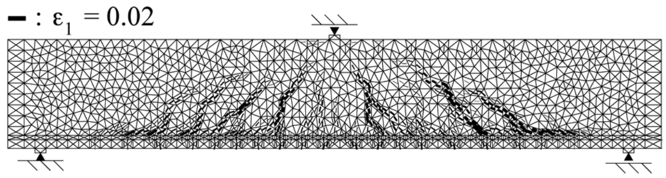

Figure 27. Cracking pattern in analysis case I05.

In Figure 22 the calculated shear response in analysis case I is compared with the experiment. Taking into account the dilatancy induced by bond slip does not result in a good estimate of the maximum shear load of the experiment. Figures 23, 24, 25, 26, and 27 are cracking patterns at maximum shear load in analysis cases I01, I02, I03, I04, and I05. In Figures 28, 29, 30, 31, and 32 the incremental displacement at the maximum shear load in analysis case I is shown together with maximum principal strain. The bond splitting cracking mechanism was expected such that the dilatancy induced by plastic slip in bond interface elements causes tensile stress and splitting cracks in concrete elements at the back of rebar plane elements. However, in analysis case I most of the splitting cracks occur at concrete elements just above the upper bond interface elements. Comparing the cracking pattern of analysis case I01 (Figs. 23 and 28) in which no dilatancy is taken into account with the one for analysis case I04 (Figs 26 and 31) assuming dilatancy, extensive bond splitting cracking and further propagation of diagonal cracks connected to the bond splitting cracks are observed in the latter case. The position of the dominant diagonal crack is much closer to the supporting plate in analysis case I04, which resembles the experiment (Fig. 1) much better than analysis case I01. The inclination angle of the dominant diagonal crack in analysis case I04 is relatively smaller compared with analysis case I01, which decreases aggregate interlock action, and results in the slight reduction of maximum shear load of the beam. In the typical diagonal tension failure experiment, the collapse mechanism completes by penetration of the diagonal crack beneath into the flexural compression part under the loading plate. A similar propagation of the diagonal crack is observed in analysis case I04.

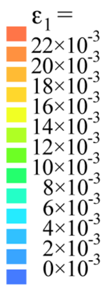

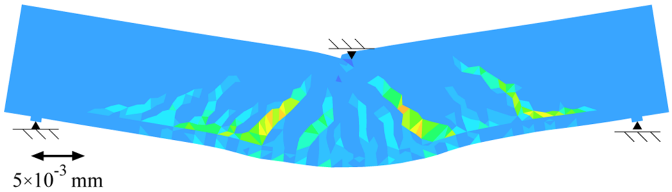

Figure 28. Incremental displacement in analysis case I01.

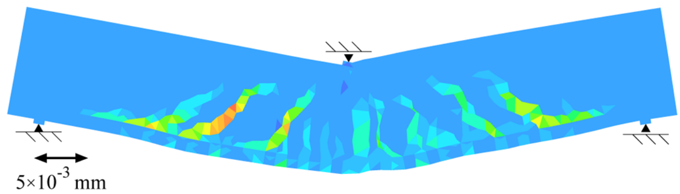

Figure 29. Incremental displacement in analysis case I02.

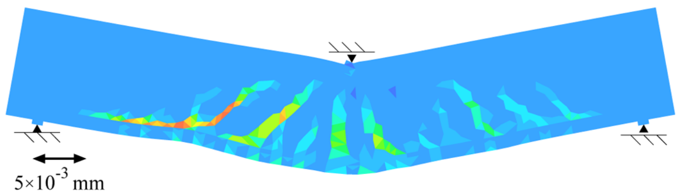

Figure 30. Incremental displacement in analysis case I03.

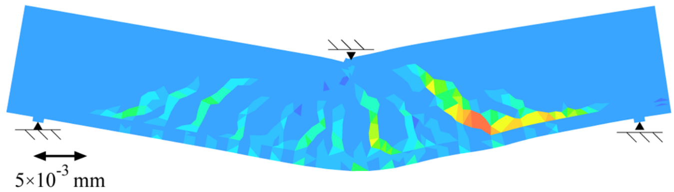

Figure 31. Incremental displacement in analysis case I04.

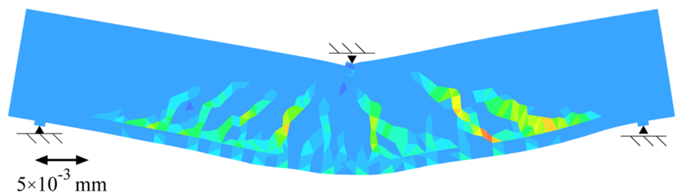

Figure 32. Incremental displacement in analysis case I05.

5 CONCLUSIONS

The influence of modeling of rebar bond slip on diagonal tension failure of reinforced concrete beams in finite element analysis was examined through calculations with several modeling strategies for bond slip and bond splitting fracture. In the first series of analysis the bond between concrete finite elements and rebar beam elements was modeled by using interface elements with average bond stress-slip relationships which are determined by solving bond slip differential-integral equations of pullout specimens with the constitutive model for bond stress-slip-rebar strain relationship. The analysis of a reinforced concrete beam showed that the bond slip modeling does not result in either widening of diagonal cracks or diagonal tension failure, but in crack dispersion and flexural failure. In the second series of analysis, another type of bond modeling used concrete and rebar beam elements disconnected partially by adopting dual nodes for them. The modeling can simulate the diagonal tension failure mode depending on the configuration of dual nodes. In the third series of analysis, the elasto-plastic constitutive model with dilatancy was assumed for bond interface elements so that the bond slip causes tensile hoop stress in concrete elements, and bond splitting cracking. Extensive bond splitting cracking and further propagation of diagonal cracks connected to the bond splitting cracks were observed in the analysis.

REFERENCES

Hasegawa, T. 1998. Multi equivalent series phase model for nonlocal constitutive relations of concrete. In H. Mihashi & K. Rokugo (eds), *Fracture Mechanics of Concrete Structures*: 1043-1054. Freiburg: AEDIFICATIO Publishers.

Hasegawa, T. 2004. Numerical study of mechanism of diagonal tension failure in reinforced concrete beams. In V. C. Li, C. K. Y. Leung, K. J. Willam, & S. L. Billington, (eds), *Fracture Mechanics of Concrete Structures*: 391-398. Ia-FraMCos, USA.

Hasegawa, T. 2007a. Finite element analysis of diagonal tension failure in RC beam. In A.Carpinteri, P.G. Gambarova, G. Ferro, & G. A. Plizzari, (eds), *Fracture Mechanics of Concrete Structures*: 709-717. Taylor & Francis Group, UK.

Hasegawa, T. 2007b. Rebar bond-slip in finite element analysis for diagonal tension failure of reinforced concrete beam. *Proc. 62nd annual conference. JSCE* 5: 703-704.

Hasegawa, T. 2008. Rebar bond modeling in finite element analysis for diagonal tension failure of reinforced concrete beam. *Proc. 63rd annual conference. JSCE* 5: 1083-1084.

Hasegawa, T. 2009. Finite element analysis for diagonal tension failure of RC beam with bond splitting fracture. *Proc. 64th annual conference. JSCE* 5: 1057-1058.

Podgorniak-Stanik, B. A. 1998. The influence of concrete strength, distribution of longitudinal reinforcement, amount of transverse reinforcement and member size on shear strength of reinforced concrete members. *M.A.S. thesis*: University of Toronto.

Shima, H., Chou, L. & Okamura, H. 1987. Micro and macro models for bond in reinforced concrete, *Journal of the Faculty of Engineering, the University of Tokyo (B)*, 39(2): 133-194.

Witte, F. & Kikstra, W. 2007. *DIANA - Finite element analysis. User's Manual release 9.2*. Delft: TNO DIANA.